

Bumpified Haar Wavelets and Tsirelson's Bound: Some Mathematical Properties and Insights from Block Toeplitz Matrices

David Dudal¹Ken Vandermeersch²¹Department of Physics, KU Leuven Campus Kortrijk – Kulak, Etienne Sabbelaan 53, 8500 Kortrijk, Belgium²Department of Mathematics, KU Leuven, Celestijnenlaan 200B, 3001 Leuven, Belgium

October 2024

Abstract

This paper investigates a recent construction using bumpified Haar wavelets to demonstrate explicit violations of the Bell-Clauser-Horne-Shimony-Holt inequality within the vacuum state in quantum field theory. The construction was tested for massless spinor fields in $(1+1)$ -dimensional Minkowski spacetime and is claimed to achieve violations arbitrarily close to an upper bound known as Tsirelson's bound. We show that this claim can be reduced to a mathematical conjecture involving the maximal eigenvalue of a sequence of symmetric matrices composed of integrals of Haar wavelet products. More precisely, the asymptotic eigenvalue of this sequence should approach π . We present a formal argument using a subclass of wavelets, allowing to reach 3.11052. Although a complete proof remains elusive, we present further compelling numerical evidence to support it.

1 Introduction

The study of Bell's inequalities has been an important topic in Quantum Mechanics since their formulation in the 1960s by John Steward Bell and others [1, 2]. A crucial aspect of understanding these inequalities is relativistic causality, which ensures that measurements made by space-like separated observers cannot influence one another. Given the role that relativistic causality plays, it seems natural to look at the Bell-CHSH inequality within the framework of Quantum Field Theory (QFT), although this introduces a few challenges.

Using the methods of Algebraic QFT, the pioneering works [4, 5, 6] have provided an existence proof—although without an explicit construction—showing that the Bell-CHSH inequality can be maximally violated at the level of free fields. Here, maximal violation means that Bell-CHSH correlations can be found arbitrarily close to Tsirelson's bound

$2\sqrt{2}$ [3]. In a recent article [12], a general setup was introduced to explicitly construct a violation of the Bell-CHSH inequality arbitrarily close to Tsirelson's bound in the vacuum state within the context of QFT. This approach was investigated in more detail for a free $(1+1)$ -dimensional massless spinor field, employing Haar wavelets, and yielded excellent numerical results.

Building on those numerical observations, in this paper we further develop the proposed construction and aim to formally prove that we can indeed get arbitrarily close to maximal violation in the special case of a free massless $(1+1)$ -dimensional spinor field. Our approach reformulates the validity of their construction, captured by Conjecture A, as a direct mathematical statement about the asymptotic behaviour of the maximal eigenvalue of a matrix formed from certain integrals of Haar wavelet products, this is Conjecture B.

Specifically, for all $n, k, m, \ell \in \mathbb{Z}$ with $k, \ell \geq 1$, we define

$$A_{(n,k),(m,\ell)} = - \iint \left(\frac{1}{x+y} \right) \psi_{n,-k}(x) \psi_{m,-\ell}(y) \, dx dy,$$

and for each $N, K \geq 1$ we consider the $(N+1)K \times (N+1)K$ matrix

$$A(N, K) = \left[A_{(n,k),(m,\ell)} \right]_{(n,k),(m,\ell)},$$

with rows indexed by

$$(n, k) = (0, 1), (0, 2), \dots, (0, K), (1, 1), (1, 2), \dots, (1, K), (2, 1), \dots$$

and similarly for the columns (m, ℓ) . We formally prove that their construction always works, *assuming* the following conjecture is true:

Conjecture B. *Given a small $\delta > 0$, we can find sufficiently large $N, K \geq 1$ such that*

$$\pi - \delta < \lambda_{\max}(A(N, K)).$$

In fact, we believe that $\lim_{N, K \rightarrow \infty} \lambda_{\max}(A(N, K)) = \pi$.

While a general proof of Conjecture B eludes us, we provide strong numerical evidence to support it.

Contents

1	Introduction	1
2	Summary of the previous paper	3

3	An exact solution in terms of wavelets (Step 1)	5
3.1	Haar wavelets	5
3.2	Problem statement	9
3.3	Numerical solution	10
3.4	Exploiting the (anti)symmetry relations	10
3.5	The matrix A	14
3.5.1	The special case $K = 1$	18
3.5.2	Outlook: The general case $K \geq 1$	26
4	Bumpification (Step 2)	29
4.1	Bumpified Haar wavelets	30
4.2	The final test functions	33

2 Summary of the previous paper

The paper [12] roughly follows the following steps, summarizing Sections V, VI and VII. We refrain from giving too many details as the focus of this paper is squarely on the mathematical properties of the proposed construction. For more details, the interested reader is referred to e.g. [15].

1. A Quantum Field Theory (QFT) for a free, $(1 + 1)$ -dimensional, spinor field is introduced, quantized using the canonical anti-commutation relations.
2. To properly define field operators in Algebraic QFT, the fields are smeared using smooth test functions with compact support. This ensures the operators are well-behaved operators acting on a Hilbert space. More specifically, for each compactly supported, smooth, two-component spinor *test function*

$$h(t, x) = (h_1(t, x), h_2(t, x))^T,$$

we can associate a well-defined *field operator* $\psi(h)$. These smeared operators respect causality, with the anti-commutator $\{\psi(h), \psi^\dagger(h')\}$ vanishing if the underlying test functions h and h' have space-like separated supports.

3. The Bell operator is then defined as $\mathcal{A}_h = \psi(h) + \psi^\dagger(h)$, which is Hermitian per construction. An inner product between test functions is defined as $\langle h | h' \rangle = \langle 0 | \mathcal{A}_h \mathcal{A}_{h'} | 0 \rangle$, the vacuum expectation value of the product $\mathcal{A}_h \mathcal{A}_{h'}$. In the special case $h = h'$, we even have that $\mathcal{A}_h^2 = \langle h | h \rangle \equiv \|h\|^2$, showing that the Bell operators are dichotomic provided the underlying test functions are normalized with respect to this inner product.

4. The Bell-CHSH correlator is then introduced as

$$\langle \mathcal{C} \rangle = \langle 0 | i [(\mathcal{A}_f + \mathcal{A}_{f'})\mathcal{A}_g + (\mathcal{A}_f - \mathcal{A}_{f'})\mathcal{A}_{g'}] | 0 \rangle,$$

where f and f' are Alice's spinor test functions and g and g' are Bob's. Their supports are located in Rindler's left and right wedges, respectively, ensuring relativistic causality.

5. By expressing the Bell-CHSH correlator in terms of the inner products of these test functions, it becomes

$$\langle \mathcal{C} \rangle = i (\langle f | g \rangle + \langle f | g' \rangle + \langle f' | g \rangle - \langle f' | g' \rangle).$$

Imposing a reality condition on the test functions and focusing only on the massless limit for now, these inner products have a nice analytical expression of the form $\langle f | g \rangle = I_1 + I_2$, where

$$\begin{aligned} I_1 &= \int \left(f_1^*(x)g_1(x) + f_2^*(x)g_2(x) \right) dx, \\ I_2 &= -\frac{i}{\pi} \iint \left(\frac{1}{x-y} \right) \left(f_1^*(x)g_1(y) - f_2^*(x)g_2(y) \right) dx dy. \end{aligned} \tag{1}$$

6. In practice, we explicitly implement relativistic causality by considering the hypersurface $t = 0$, or better said, the temporal part of all test functions are considered to be of the type $\varepsilon^{-1}\beta(t\varepsilon^{-1})$, with $\beta(t)$ a bump function of choice, normalized to 1. For $\varepsilon \rightarrow 0^+$, this corresponds to multiplication with a Dirac- $\delta(t)$. We can then simply restrict the supports of the remaining spatial part of the test functions, namely Alice's (f, f') to $x < 0$, and Bob's (g, g') to $x > 0$.

This sets up the mathematical framework needed to investigate possible violations of Bell's inequalities: we need to find test functions (f, f') for Alice and (g, g') for Bob such that

$$2 < |\langle \mathcal{C} \rangle| < 2\sqrt{2}.$$

In particular, we are interested in constructing test functions such that the inequality is maximally violated. That is, violations arbitrarily close to Tsirelson's bound:

$$|\langle \mathcal{C} \rangle| \rightarrow 2\sqrt{2} \approx 2.83.$$

To achieve this, the following strategy is used: take $\eta \in (\sqrt{2}-1, 1)$ as a given parameter (denoted λ in the previous paper [12]) and see if we can find a solution to the equations

$$\langle f | g \rangle = \langle f' | g \rangle = \langle f | g' \rangle = -\langle f' | g' \rangle = -i \frac{\sqrt{2}\eta}{1+\eta^2}.$$

If yes, it is easily checked that then $|\langle \mathcal{C} \rangle| = \frac{4\sqrt{2}\eta}{1+\eta^2} \in (2, 2\sqrt{2})$ with $|\langle \mathcal{C} \rangle| \rightarrow 2\sqrt{2}$ as $\eta \rightarrow 1$. Concretely, this is done in two steps:

- **Step 1.** We start by solving the system of equations for a set of preliminary test functions (\tilde{f}, \tilde{f}') and (\tilde{g}, \tilde{g}') , using a finite series representation of *Haar wavelets*. This leads to piecewise constant functions, allowing the integrals in the calculations to be evaluated exactly. [12, Section VIII]
- **Step 2.** These Haar wavelets are then smoothed (bumpified) into continuous and differentiable versions. This bumpification ensures the final test functions are consistent with the smoothness requirements of Algebraic QFT. [12, Section IX]

In Section 3, after briefly introducing the Haar wavelet basis and discussing a few relevant properties, we investigate Step 1, illustrating that the equations can be solved *exactly* provided the (finite) family of Haar wavelets is taken sufficiently large—this is the most challenging part of the process. Finally, in Section 4, we explain why Step 2 works, provided we have already solved for the preliminary set of test functions from Step 1.

3 An exact solution in terms of wavelets (Step 1)

3.1 Haar wavelets

Following [12, Section VIII], we employ Haar wavelets to construct the necessary test functions. Haar wavelets [17] are a special type of Daubechies wavelets [7], used widely in signal processing and data compression [16].

Definition 3.1 (Haar wavelets). The *mother Haar wavelet* with support on the interval $[0, 1]$ is defined by

$$\psi(x) = \begin{cases} +1 & \text{if } 0 \leq x < \frac{1}{2} \\ -1 & \text{if } \frac{1}{2} \leq x < 1 \\ 0 & \text{otherwise.} \end{cases}$$

For every pair of integers n and k the Haar wavelet $\psi_{n,k}$ is supported on the half-open interval $I_{n,k} = [k2^{-n}, (k+1)2^{-n})$ and is defined by

$$\psi_{n,k}(x) = 2^{n/2} \psi(2^n x - k).$$

Thus, the (n, k) th Haar wavelet $\psi_{n,k}$ is a piecewise constant function, taking the value $+2^{n/2}$ on the first half of the interval $I_{n,k}$ and $-2^{n/2}$ on the second half, being a rescaling of the mother Haar wavelet ψ .

The family of Haar wavelets $\{\psi_{n,k}\}_{n,k \in \mathbb{Z}}$ is an *orthonormal basis* for the space of square integrable functions $L^2(\mathbb{R})$; that is, the orthogonality condition

$$\int \psi_{n,k}(x) \psi_{m,\ell}(x) dx = \delta_{n,k} \delta_{m,\ell}$$

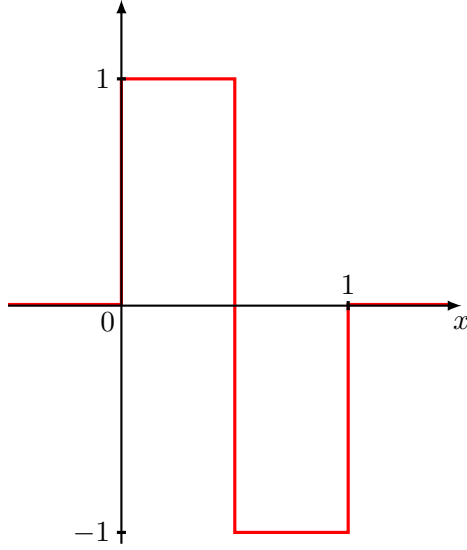


Figure 1: The mother Haar wavelet $\psi = \psi_{0,0}$.

is satisfied *and* the linear span of $\{\psi_{n,k}\}_{n,k \in \mathbb{Z}}$ is dense in $L^2(\mathbb{R})$. [17]

The following symmetry property will be very useful to us.

Lemma 3.2. *For all $n, k \in \mathbb{Z}$ we have*

$$\psi_{n,k}(-x) = -\psi_{n,-k-1}(x) \text{ almost everywhere.}$$

Proof. We start by noting that the property holds for the mother Haar wavelet $\psi = \psi_{0,0}$. Indeed,

$$\begin{aligned} \psi_{0,0}(-x) &= \psi(-x) \\ &= \begin{cases} +1 & \text{if } 0 \leq -x < \frac{1}{2} \\ -1 & \text{if } \frac{1}{2} \leq -x < 1 \\ 0 & \text{otherwise} \end{cases} \\ &= \begin{cases} -(-1) & \text{if } \frac{1}{2} < x + 1 \leq 1 \\ -(+1) & \text{if } 0 < x + 1 \leq \frac{1}{2} \\ 0 & \text{otherwise,} \end{cases} \end{aligned}$$

which equals $-\psi_{0,-1}(x) = -\psi(x + 1)$ everywhere except in the three points of discontinuity, and hence, almost everywhere. As a consequence, for all $n, k \in \mathbb{Z}$ we have

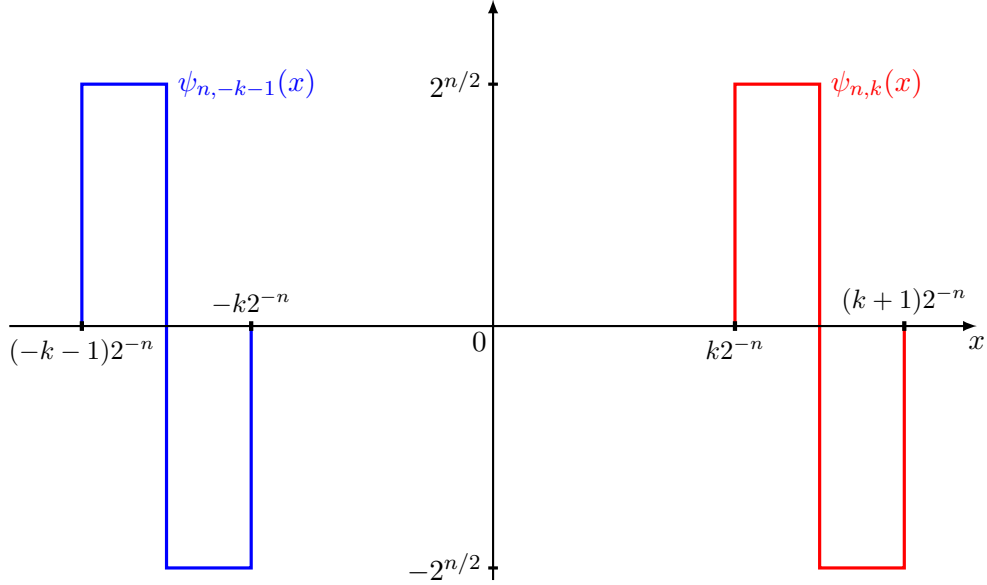


Figure 2: The a.e. equality $\psi_{n,k}(-x) = -\psi_{n,-k-1}(x)$, visually.

that

$$\begin{aligned}
\psi_{n,k}(-x) &= \begin{cases} 2^{n/2} \psi(2^n(-x) - k) & \text{if } -x \in I_{n,k} \\ 0 & \text{otherwise} \end{cases} \\
&= \begin{cases} -2^{n/2} \psi(2^n x + k + 1) & \text{if } x \in I_{n,-k-1} \\ 0 & \text{otherwise} \end{cases} \\
&= -\psi_{n,-k-1}(x)
\end{aligned}$$

holds almost everywhere. See also Fig. 2 for an intuitive visualization. \square

We will study certain integrals containing these Haar wavelets and they will have the following form:

Notation 3.3. For all $n, k, m, \ell \in \mathbb{Z}$ with $k, \ell \geq 1$, we define

$$A_{(n,k),(m,\ell)} = - \iint \left(\frac{1}{x+y} \right) \psi_{n,-k}(x) \psi_{m,-\ell}(y) \, dx dy.$$

Lemma 3.4. For all $n, k, m, \ell \in \mathbb{Z}$ with $k, \ell \geq 1$, we have $A_{(n,k),(m,\ell)} > 0$.

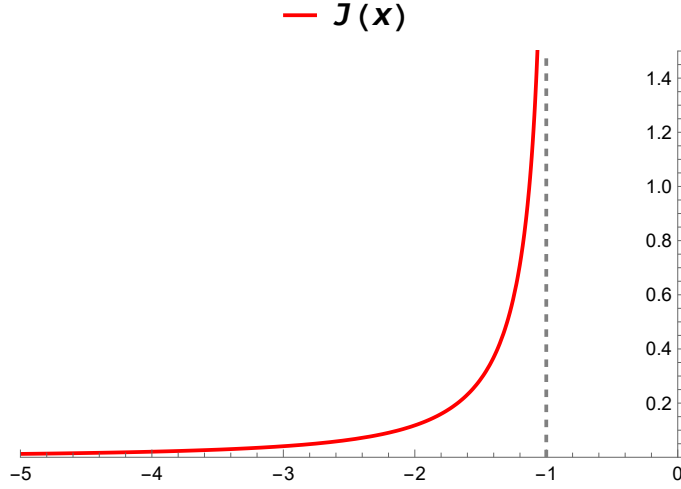


Figure 3: The graph of the function J from the proof of Lemma 3.4.

Proof. Let us rewrite the given integral by first integrating with respect to x :

$$A_{(n,k),(m,\ell)} = - \int \psi_{m,-\ell}(y) \left(\int \frac{\psi_{n,-k}(x)}{x+y} dx \right) dy.$$

Then, for each $y < 0$ we can compute the inner integral as

$$\begin{aligned} I(y) &:= \int \frac{\psi_{n,-k}(x)}{x+y} dx = \int_{-k2^{-n}}^{(-k+\frac{1}{2})2^{-n}} \frac{+2^{n/2}}{x+y} dx + \int_{(-k+\frac{1}{2})2^{-n}}^{(-k+1)2^{-n}} \frac{-2^{n/2}}{x+y} dx \\ &= 2^{n/2} \ln \left(\frac{(-k+\frac{1}{2})2^{-n} + y}{-k2^{-n} + y} \right) - 2^{n/2} \ln \left(\frac{(-k+1)2^{-n} + y}{(-k+\frac{1}{2})2^{-n} + y} \right). \end{aligned}$$

Now remark that the function $I: (-\infty, 0) \rightarrow \mathbb{R}$ is strictly increasing. Indeed, we may write $I(y) = 2^{n/2} J(2^n y - k)$ where $J: (-\infty, -k) \subset (-\infty, -1) \rightarrow \mathbb{R}$ is defined by

$$J(x) = \ln \left(\frac{\frac{1}{2} + x}{x} \right) - \ln \left(\frac{1+x}{\frac{1}{2} + x} \right) = \ln \left(\frac{(\frac{1}{2} + x)^2}{x(1+x)} \right)$$

and where $\frac{(\frac{1}{2} + x)^2}{x(1+x)}$ can be easily verified to be strictly increasing for $x < -1$. The graph of the function J function is depicted in Fig. 3.

It follows that

$$\begin{aligned} A_{(n,k),(m,\ell)} &= - \int \psi_{m,-\ell}(y) I(y) \, dy. \\ &= -2^{m/2} \int_{-\ell 2^{-m}}^{(-\ell + \frac{1}{2})2^{-m}} I(y) \, dy + 2^{m/2} \int_{(-\ell + \frac{1}{2})2^{-m}}^{(-\ell + 1)2^{-m}} I(y) \, dy > 0. \end{aligned}$$

□

Remark 3.5. The function J defined in the proof of Lemma 3.4 will come back in later parts of this work. As stated in the proof, it is strictly increasing. It can also be verified that it is a strictly positive function and that it defines a bijection $(-\infty, -1) \rightarrow (0, \infty)$.

3.2 Problem statement

Resuming from Section 2, we employ these Haar wavelets to solve the following system of equations:

$$\begin{aligned} \langle \tilde{f} \mid \tilde{f} \rangle &= \langle \tilde{f}' \mid \tilde{f}' \rangle = \langle \tilde{g} \mid \tilde{g} \rangle = \langle \tilde{g}' \mid \tilde{g}' \rangle = 1 \\ \langle \tilde{f} \mid \tilde{g} \rangle &= \langle \tilde{f}' \mid \tilde{g} \rangle = \langle \tilde{f} \mid \tilde{g}' \rangle = -\langle \tilde{f}' \mid \tilde{g}' \rangle = -i \frac{\sqrt{2}\eta}{1 + \eta^2}. \end{aligned} \quad (2)$$

Here, $\eta \in (\sqrt{2} - 1, 1)$ is a given parameter. (This corresponds to [12, Eq. (28)] that the original authors solve numerically.) These initial test functions are expanded as finite linear combinations of the Haar wavelets,

$$\begin{aligned} \tilde{f}_j &:= \sum_{n=N_0}^{N_1} \sum_{k=-K}^{-1} f_j(n, k) \psi_{n,k}, & \tilde{g}_j &:= \sum_{n=N_0}^{N_1} \sum_{k=0}^{K-1} g_j(n, k) \psi_{n,k}, \\ \tilde{f}'_j &:= \sum_{n=N_0}^{N_1} \sum_{k=-K}^{-1} f'_j(n, k) \psi_{n,k}, & \tilde{g}'_j &:= \sum_{n=N_0}^{N_1} \sum_{k=0}^{K-1} g'_j(n, k) \psi_{n,k}, \end{aligned} \quad (3)$$

for $j \in \{1, 2\}$, so that, after substituting these expansions, we only need to solve the system of equations (2) for the finite set of wavelet coefficients $f_j(n, k)$, $g_j(n, k)$, $f'_j(n, k)$, $g'_j(n, k)$.

The parameters $N_0 < N_1$ and $K > 1$ set the resolution; increasing the resolution results in more Haar wavelets being used and the system of equations (2) thus becoming easier to solve. The idea will be that, for a given $\eta \in (\sqrt{2} - 1, 1)$ *arbitrarily close* to 1, we can find a resolution *sufficiently fine* such that the system of equations (2) has an *exact* solution for the wavelet coefficients. We note that the causality condition is implemented by only using Haar wavelets supported on $[-2^{-N_0}K, 0)$ to represent Bob's test functions f, f' and only using Haar wavelets supported on $[0, 2^{-N_0}K)$ to represent Alice's test functions g, g' . [12, Section VIII]

The following conjecture states that this procedure always works and we spend the rest of this section providing evidence for it.

Conjecture A. *Given any $\eta \in (\sqrt{2} - 1, 1)$, a resolution $\{N_0, N_1, K\}$ can be found such that the system of equations (2) admits a solution of the form (3).*

From [12, Eqs. (26), (27)], we know that substituting the expansions (3) into the considered norms and inner products (1) yields expressions of the form

$$\langle \tilde{f} | \tilde{f} \rangle = \sum_{n,k} (f_1(n,k)^2 + f_2(n,k)^2) \quad (4)$$

and

$$\begin{aligned} \langle \tilde{f} | \tilde{g} \rangle &= \sum_{n,k,m,\ell} \left(f_1(n,k)g_1(m,\ell) - f_2(n,k)g_2(m,\ell) \right) \\ &\quad \times \left(-\frac{i}{\pi} \iint \left(\frac{1}{x-y} \right) \psi_{n,k}(x)\psi_{m,\ell}(y) \, dx dy \right), \end{aligned} \quad (5)$$

where both sums are finite and depend on the resolution. Of course, similar expressions hold for the other norms and inner products entering the system of equations (2).

3.3 Numerical solution

The authors of [12] then proceeded to numerically solve the system of equations (2) for the unknown wavelet coefficients, considering two cases: $\eta = 0.7$ and $\eta = 0.99$, which yielded corresponding correlations $|\langle \mathcal{C} \rangle| \approx 2.66$ and $|\langle \mathcal{C} \rangle| \approx 2.82$, both already quite close to maximal violation. Bumpified versions of these test functions were subsequently found with numerically indistinguishable violations. The final test functions corresponding to $\eta = 0.99$ are depicted in Fig. 4, a copy of Fig. 2 from the previous paper [12].

The graphs of these functions seem to exhibit a number of (anti)symmetry relations which we intend to exploit to simplify the system of equations (2). Doing this, we can convert Conjecture A to a more direct mathematical statement, Conjecture B, concerning the maximal eigenvalue of a certain matrix.

3.4 Exploiting the (anti)symmetry relations

Consider the expressions for the inner products (5). Applying a change of variables $(x, v) \leftarrow (x, -y)$ and using the a.e. equality of Lemma 3.2, we can rewrite them as follows:

$$\begin{aligned} \iint \left(\frac{1}{x-y} \right) \psi_{n,k}(x)\psi_{m,\ell}(y) \, dx dy &= \iint \left(\frac{1}{x+v} \right) \psi_{n,k}(x)\psi_{m,\ell}(-v) \, dx dv \\ &= - \iint \left(\frac{1}{x+v} \right) \psi_{n,k}(x)\psi_{m,-\ell-1}(v) \, dx dv \\ &\equiv A_{(n,-k),(m,\ell+1)}. \end{aligned} \quad (\text{by Notation 3.3})$$

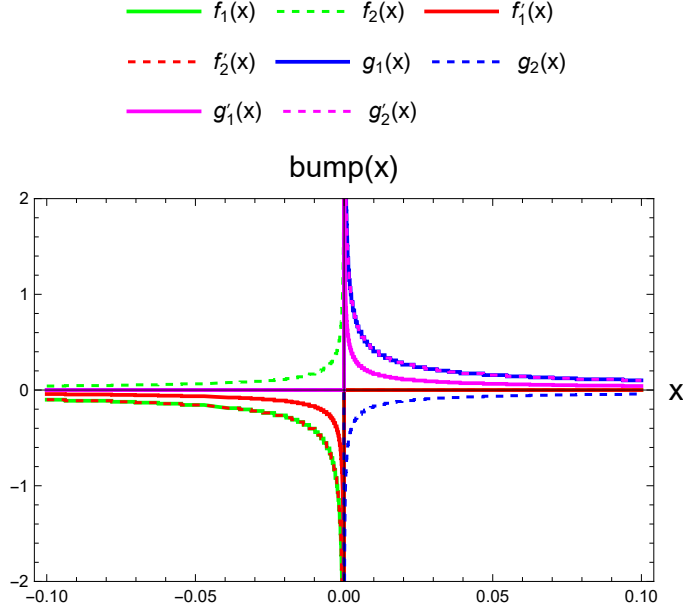


Figure 4: Fig. 2 in [12]: Test function components for $\eta = 0.99$ where the resolution was set to $N_0 = -10$, $N_1 = 120$, $K = 5$.

Hence, after reindexing the summations in Eq. (5) by $k \leftarrow -k$ and $\ell \leftarrow \ell + 1$ (so that k and ℓ both run over the range $\{1, \dots, K\}$), we find

$$\langle \tilde{f} | \tilde{g} \rangle = -\frac{i}{\pi} \sum_{n,k,m,\ell} A_{(n,k),(m,\ell)} \left(f_1(n, -k) g_1(m, \ell - 1) - f_2(n, -k) g_2(m, \ell - 1) \right),$$

with similar expressions for the other inner products.

Now, we proceed to simplify the problem statement (2) significantly, reducing the number of coefficients that we need to solve for by imposing three extra constraints that we can observe in Fig. 4 ([12, Fig. 2]).

1. First, we note from Fig. 4 that $f_2' = f_1$ and $f_1' = -f_2$ for Alice's spinor test functions, with similar expressions holding for Bob's. Hence, it makes sense to assume that the solution satisfies

$$\begin{aligned} f_2'(n, k) &= f_1(n, k), & f_1'(n, k) &= -f_2(n, k), \\ g_2'(n, k) &= g_1(n, k), & g_1'(n, k) &= -g_2(n, k). \end{aligned}$$

It can then be verified that the required equalities $\langle \tilde{f} | \tilde{g} \rangle = -\langle \tilde{f}' | \tilde{g}' \rangle$ and $\langle \tilde{f}' | \tilde{g} \rangle = \langle \tilde{f} | \tilde{g}' \rangle$

$\tilde{g}\rangle = \langle \tilde{f} | \tilde{g}'\rangle$ in (2) follow directly. For example, the first equality follows from

$$\begin{aligned} f_1'(n, -k)g_1'(m, \ell - 1) - f_2'(n, -k)g_2'(m, \ell - 1) \\ &= f_2(n, -k)g_2(m, \ell - 1) - f_1(n, -k)g_1(m, \ell - 1) \\ &= -\left(f_1(n, -k)g_1(m, \ell - 1) - f_2(n, -k)g_2(m, \ell - 1)\right). \end{aligned}$$

2. Another antisymmetry relation that can be observed from Fig. 4 is that $f(-x) = -g(x)$. This relation can be enforced by imposing

$$g_1(n, k) = f_1(n, -k - 1) \quad \text{and} \quad g_2(n, k) = f_2(n, -k - 1).$$

Indeed, by Lemma 3.2, we then find that

$$\begin{aligned} f_j(-x) &= \sum_{n=N_0}^{N_1} \sum_{k=1}^K f_j(n, -k) \psi_{n, -k}(-x) \\ &= - \sum_{n=N_0}^{N_1} \sum_{k=1}^K g_j(n, k - 1) \psi_{n, k-1}(x) \\ &= -g_j(x), \end{aligned}$$

almost everywhere.

3. Lastly, again based on Fig. 4, it seems plausible that $f_2 = -cf_1$ for some constant $0.25 < c < 0.5$. Hence it makes sense to impose $f_2(n, k) = -cf_1(n, k)$, where c is yet to be determined.

Under these three extra assumptions, Conjecture A simplifies to finding a resolution $\{N_0, N_1, K\}$ such that the following system of equations:

$$\begin{aligned} \sum_{n,k,m,\ell} A_{(n,k),(m,\ell)} \left(f_1(n, -k)f_1(m, -\ell) - c^2 f_1(n, -k)f_1(m, -\ell) \right) &= \frac{\pi\sqrt{2}\eta}{1 + \eta^2} \\ \sum_{n,k,m,\ell} A_{(n,k),(m,\ell)} \left(-cf_1(n, -k)f_1(m, -\ell) - cf_1(n, -k)f_1(m, -\ell) \right) &= -\frac{\pi\sqrt{2}\eta}{1 + \eta^2}, \end{aligned}$$

admits an exact solution satisfying the normality condition

$$\sum_{n,k} f_1(n, -k)^2 + c^2 f_1(n, -k)^2 = 1.$$

For brevity, let us agree to write $x_{n,k} := f_1(n, -k)$ for all $N_0 \leq n \leq N_1$ and $1 \leq k \leq K$. We may put these unknowns in a vector x indexed by these (n, k) , ordered as follows:

$$x = \left[x_{N_0,1} \quad \cdots \quad x_{N_0,K} \mid x_{N_0+1,1} \quad \cdots \quad x_{N_1-1,K} \mid x_{N_1,1} \quad \cdots \quad x_{N_1,K} \right]^T \in \mathbb{R}^d,$$

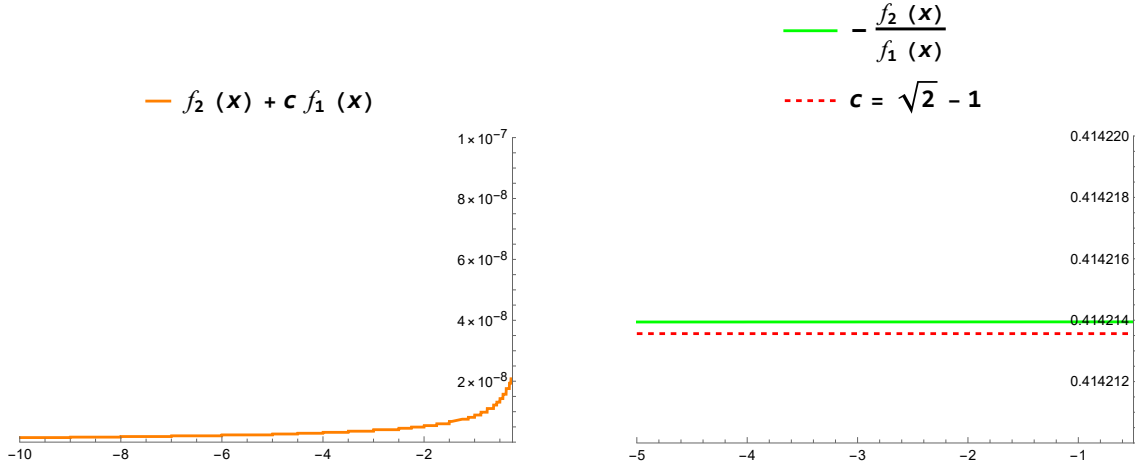


Figure 5: The test function components of $f = (f_1, f_2)$ found in [12] satisfy the relation $f_2 = -cf_1$ quite closely.

where $d = (N_1 - N_0 + 1) \times K$. Then, the problem statement compactifies to

$$(1 - c^2) \sum_{n,k,m,\ell} A_{(n,k),(m,\ell)} x_{n,k} x_{m,\ell} = \frac{\pi\sqrt{2}\eta}{1 + \eta^2} \quad (6)$$

$$-2c \sum_{n,k,m,\ell} A_{(n,k),(m,\ell)} x_{n,k} x_{m,\ell} = -\frac{\pi\sqrt{2}\eta}{1 + \eta^2}, \quad (7)$$

and the normality condition on f becomes the following normality condition on x :

$$\|x\|^2 = 1/(1 + c^2).$$

A natural first step towards a solution to this system of equations is to add both equations (6) + (7) together, obtaining

$$(1 - 2c - c^2) \sum_{n,k,\ell,m} A_{(n,k),(m,\ell)} x_{n,k} x_{m,\ell} = 0.$$

This equation can be satisfied by simply taking c as the positive root of the quadratic polynomial $1 - 2x - x^2$, namely $c = \sqrt{2} - 1 \approx 0.4142$.

Remark 3.6. We note the excellent agreement between this value for c and the one obtained numerically by using the test functions corresponding to $\eta = 0.99$ found in [12]. The components of the final test function $f = (f_1, f_2)$ should approximately satisfy $f_2 = -cf_1$, where $c = \sqrt{2} - 1$. Fig. 5 appears to verify this, where the graphs of both $f_2 + cf_1 \approx 0$ and $-f_2/f_1 \approx c$ are depicted.

Next, as we require the unknown vector x to satisfy $\|x\|^2 = 1/(1+c^2)$, it makes sense to rescale the set of unknowns by looking for a vector of the form

$$y := \sqrt{1+c^2} x,$$

which is normalized. Accordingly, “all” we still have to do now is solve

$$\sum_{(n,k)} \sum_{(m,\ell)} A_{(n,k),(m,\ell)} y_{n,k} y_{m,\ell} = \frac{1+c^2}{1-c^2} \times \frac{\pi\sqrt{2}\eta}{1+\eta^2} = \frac{2\pi\eta}{1+\eta^2},$$

such that $\|y\|^2 = 1$.

3.5 The matrix A

In a similar fashion to how we define the vectors x and y , we can define the $d \times d$ symmetric matrix

$$A = [A_{(n,k),(m,\ell)}]_{(n,k),(m,\ell)},$$

with entries given by Notation 3.3, further compactifying the problem statement. In the previous subsection, we have demonstrated that Conjecture A can be reduced to the following statement:

We have to find a solution $y \in \mathbb{R}^d$ to

$$y^\top A y = \frac{2\pi\eta}{1+\eta^2} \quad \text{such that} \quad \|y\|^2 = 1. \quad (8)$$

The existence of such a vector depends on the eigenvalues of A , which, in turn, depend on the parameters N_0 , N_1 and K . By the spectral theorem, we can decompose A as

$$A = Q \begin{bmatrix} \lambda_1 & & & \\ & \lambda_2 & & \\ & & \ddots & \\ & & & \lambda_d \end{bmatrix} Q^\top,$$

where Q is an orthogonal matrix and $\lambda_d \leq \dots \leq \lambda_2 \leq \lambda_1$ are the ordered eigenvalues of A . For the extremal eigenvalues, we also write $\lambda_{\max} := \lambda_1$ and $\lambda_{\min} := \lambda_d$.

Proposition 3.7. *The problem statement (8) has a solution if and only if*

$$\lambda_{\min} \leq \frac{2\pi\eta}{1+\eta^2} \leq \lambda_{\max}.$$

0.340	0.0179	0.00490	0.321	0.0284	0.00919	0.274	0.0360	0.0139,
0.0179	0.00490	0.00202	0.00919	0.00414	0.00222	0.00405	0.00256	0.00173,
0.00490	0.00202	0.00102	0.00222	0.00133	0.000857	0.000899	0.000679	0.000526,
0.321	0.00919	0.00222	0.340	0.0179	0.00490	0.321	0.0284	0.00919,
0.0284	0.00414	0.00133	0.0179	0.00490	0.00202	0.00919	0.00414	0.00222,
0.00919	0.00222	0.000857	0.00490	0.00202	0.00102	0.00222	0.00133	0.000857,
0.274	0.00405	0.000899	0.321	0.00919	0.00222	0.340	0.0179	0.00490,
0.0360	0.00256	0.000679	0.0284	0.00414	0.00133	0.0179	0.00490	0.00202,
0.0139	0.00173	0.000526	0.00919	0.00222	0.000857	0.00490	0.00202	0.00102

Table 1: The matrix $A(2, 3)$. Notice the $K \times K$ block structure.

Proof. It follows from the Rayleigh-Ritz theorem that the image of the unit sphere $S^{d-1} \subset \mathbb{R}^d$ under the quadratic form $q(x) = x^\top A x$ equals the closed interval

$$q(S^{d-1}) = [\lambda_{\min}, \lambda_{\max}],$$

which is equivalent to what we have to show. \square

Interestingly, the matrix A depends only on the difference $N := N_1 - N_0$. This follows from the observation that

$$A_{(n+1,k),(m+1,\ell)} = A_{(n,k),(m,\ell)},$$

for all $n, m \in \mathbb{Z}$, $k, \ell \in \mathbb{Z}_{\geq 1}$. As a result, to study the spectrum of A , we can set $N_0 = 0$ and $N_1 = N$ without loss of generality. To emphasize this dependence, we also write $A(N, K)$ instead of A . As an example, Table 1 shows the matrix $A(2, 3)$, i.e., the matrix A for $N = 2$ and $K = 3$.

We are particularly interested in the behavior as $\eta \rightarrow 1$, where $\frac{2\pi\eta}{1+\eta^2} \rightarrow \pi$. This suggests that we should be able to make the largest eigenvalue $\lambda_{\max}(A(N, K)) = \|A(N, K)\|_2$ approach π by taking the resolution N , K sufficiently large. Numeric results support this expectation: this can be seen in Fig. 6, where we have depicted discrete plots of $\|A(N, K)\|_2$ for $2 \leq N \leq 50$, once for $K = 2$ and once for $K = 5$.

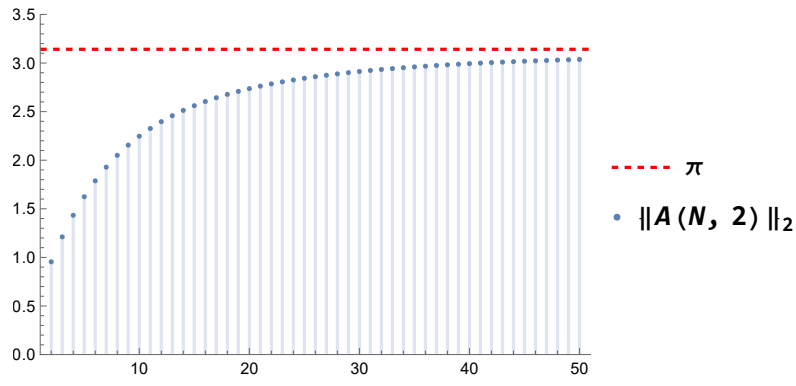
Remark 3.8 (Minimal eigenvalue). As we are particularly interested in the behavior as $\eta \rightarrow 1$, the **minimal** eigenvalue of the matrix $A(N, K)$ plays only a minor role. Indeed, for any $N, K \geq 1$, we can guarantee that

$$\lambda_{\min}(A(N, K)) \leq A_{(0,1),(0,1)} = \ln\left(\frac{1024}{729}\right) \approx 0.340.$$

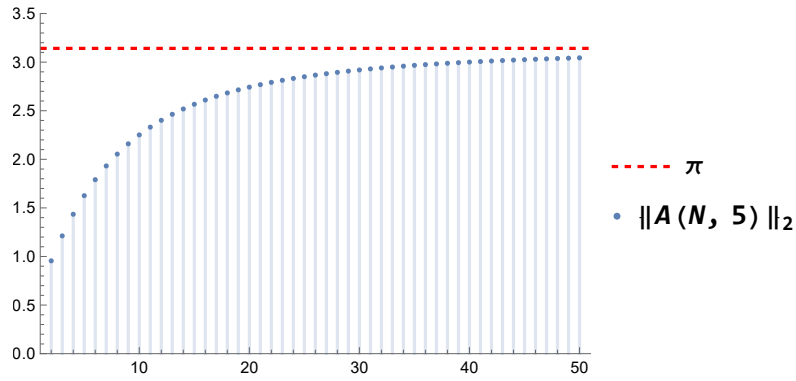
This inequality holds because $A_{(0,1),(0,1)}$ is a diagonal entry of the symmetric matrix $A(N, K)$, and thus must be greater than or equal to the minimal eigenvalue.¹ Hence, the

¹To see why this is the case, consider the inequality

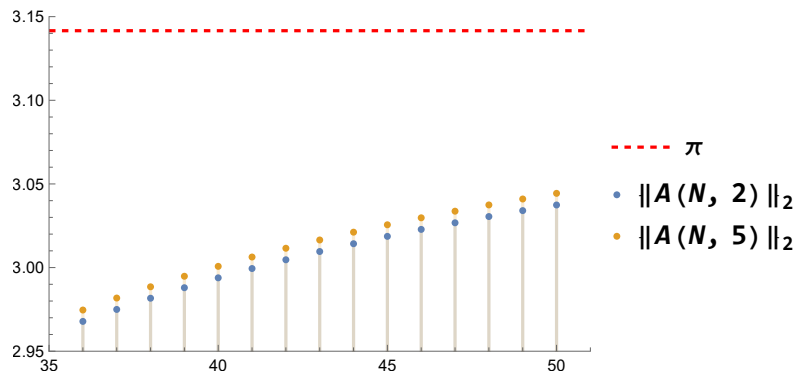
$$\forall y \in \mathbb{R}_{\neq 0}^d: \quad \lambda_{\min}(A(N, K)) \leq \frac{y^\top A(N, K)y}{y^\top y}$$



(a) $\lambda_{\max}(A(N, 2))$ as a function of N



(b) $\lambda_{\max}(A(N, 5))$ as a function of N



(c) Comparing $\lambda_{\max}(A(N, 2))$ and $\lambda_{\max}(A(N, 5))$

Figure 6: Discrete plots for $\lambda_{\max}(A(N, 2))$ and $\lambda_{\max}(A(N, 5))$, together with a comparison.

lower bound in Proposition 3.7 is satisfied by default, since

$$\min_{\eta \in [\sqrt{2}-1, 1]} \frac{2\pi\eta}{1+\eta^2} = \frac{2\pi(\sqrt{2}-1)}{1+(\sqrt{2}-1)^2} \approx 2.22.$$

Let us formally state our conjecture concerning the maximal eigenvalue of the matrix $A(N, K)$.

Conjecture B. *Given a small $\delta > 0$, we can find sufficiently large $N, K \geq 1$ such that*

$$\pi - \delta < \lambda_{\max}(A(N, K)).$$

In particular, this implies that given $\eta \in (\sqrt{2}-1, 1)$ close to 1, we can find sufficiently large $N, K \geq 1$ such that

$$\frac{2\pi\eta}{1+\eta^2} \leq \lambda_{\max}(A(N, K)).$$

We have demonstrated that Conjecture B is sufficient to prove our earlier hypothesis Conjecture A.

Proposition 3.9. *Conjecture B \implies Conjecture A.*

Remark 3.10. In fact, Conjecture B is equivalent to

$$\lim_{N, K \rightarrow \infty} \lambda_{\max}(A(N, K)) = \pi.$$

This is because:

- Once we have found $N, K \geq 1$ such that $\pi - \delta < \lambda_{\max}(A(N, K))$, then also $\pi - \delta < \lambda_{\max}(A(N', K'))$ for each $N' \geq N$ and each $K' \geq K$. This is because $A(N, K)$ is a submatrix of $A(N', K')$.
- $\lambda_{\max}(A(N, K)) \leq \pi$ as otherwise a solution could be found which would violate the Tsirelson bound in free QFT [3, 6, 4, 5]).

Returning to the example in Table 1 ($N = 2, K = 3$), by subdividing the matrix into $K \times K$ blocks, we notice that $A(N, K)$ is *block Toeplitz*. This means that the matrix $A(N, K)$ is of the following form:

$$A = \begin{bmatrix} A_0 & A_1^\top & A_2^\top \\ A_1 & A_0 & A_1^\top \\ A_2 & A_1 & A_0 \end{bmatrix}.$$

This is the case for general N and K .

(another consequence of Rayleigh-Ritz) and plug in the first basis vector $y = [1 \ 0 \ \dots]^\top$.

Proposition 3.11. *The symmetric matrix $A(N, K)$ is block Toeplitz: visually, we have*

$$A = \begin{bmatrix} A_0 & A_1^\top & A_2^\top & \cdots & A_N^\top \\ A_1 & A_0 & A_1^\top & \cdots & A_{N-1}^\top \\ A_2 & A_1 & A_0 & \cdots & A_{N-2}^\top \\ \vdots & \vdots & \vdots & \ddots & \vdots \\ A_N & A_{N-1} & A_{N-2} & \cdots & A_0 \end{bmatrix},$$

where the individual blocks $A_0(K), \dots, A_N(K)$ are of size $K \times K$ and of the form

$$A_n(K) = \left[A_{(n,k),(0,\ell)} \right]_{\substack{1 \leq k \leq K \\ 1 \leq \ell \leq K}}$$

Proof of Proposition 3.11. We already know that the matrix $A(N, K)$ is symmetric, so we only have to check that the blocks satisfy the Toeplitz structure. By the definition of $A(N, K)$, it follows that the blocks are indexed by (n, m) : for example, for $N = 3$, the block indices are given by:

$$\begin{bmatrix} (0, 0) & (0, 1) & (0, 2) & (0, 3) \\ (1, 0) & (1, 1) & (1, 2) & (1, 3) \\ (2, 0) & (2, 1) & (2, 2) & (2, 3) \\ (3, 0) & (3, 1) & (3, 2) & (3, 3) \end{bmatrix}.$$

while the matrix elements inside of each block (n, m) are indexed by (k, ℓ) . The matrix being block Toeplitz now follows from the earlier observation that

$$A_{(n+1,k),(m+1,\ell)} = A_{(n,k),(m,\ell)},$$

for all $n, m \in \mathbb{Z}$, $k, \ell \in \mathbb{Z}_{\geq 1}$. Indeed, this shows that the blocks indexed by (n, m) and $(n + 1, m + 1)$ are always equal; that is, blocks down the same diagonal are equal. \square

3.5.1 The special case $K = 1$

As the matrix $A(N, K)$ is block Toeplitz with blocks of size $K \times K$, it makes sense to start by studying the case $K = 1$. Then, the matrix $A(N, 1)$ is just a real symmetric $(N + 1) \times (N + 1)$ Toeplitz matrix. That is, A is of the following form:

$$A = \begin{bmatrix} a_0 & a_1 & a_2 & \cdots & a_N \\ a_1 & a_0 & a_1 & \cdots & a_{N-1} \\ a_2 & a_1 & a_0 & \cdots & a_{N-2} \\ \vdots & \vdots & \vdots & \ddots & \vdots \\ a_N & a_{N-1} & a_{N-2} & \cdots & a_0 \end{bmatrix},$$

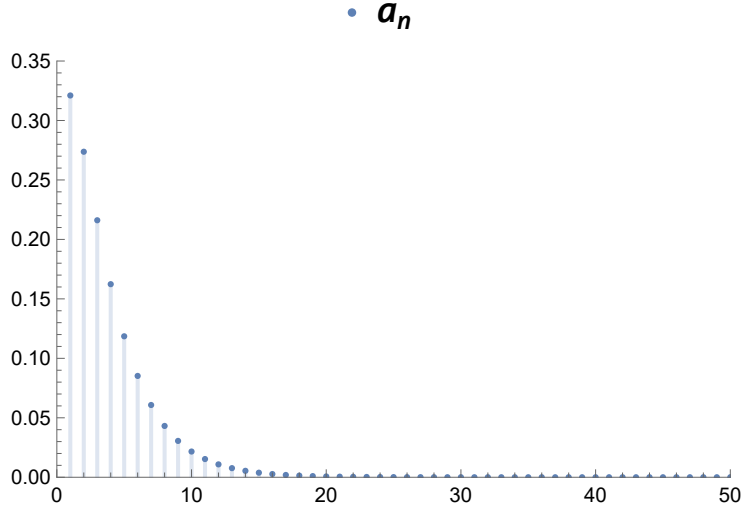


Figure 7: The terms a_n vanish relatively quickly.

where the sequence a_0, a_1, a_2, \dots is given by (see the proof of Lemma 3.4)

$$a_n = A_{(0,1),(n,1)} = -2^{n/2} \int_{-2^{-n}}^{-2^{-n-1}} J(y-1) dy + 2^{n/2} \int_{-2^{-n-1}}^0 J(y-1) dy.$$

The following closed form expression can be obtained:

$$a_n = 2^{-n/2} \left((2^{n+1} - 2^n) \ln(2) - 2(2^{n-1} + 1) \ln(2^{n-1} + 1) + 3(2^n + 1) \ln(2^n + 1) - (2^{n+1} + 1) \ln(2^{n+1} + 1) \right).$$

It can be proved that this sequence decreases in a_n and that $a_n \rightarrow 0$ as $n \rightarrow \infty$. See also Fig. 7 for some visual evidence of this.

For real symmetric Toeplitz matrices, we can prove the following result:

Proposition 3.12. *Let $(a_n)_{n \geq 0}$ be an absolutely summable sequence of real numbers and define an associated sequence of real symmetric Toeplitz matrices*

$$A_n = \begin{bmatrix} a_0 & a_1 & a_2 & \cdots & a_n \\ a_1 & a_0 & a_1 & \cdots & a_{n-1} \\ a_2 & a_1 & a_0 & \cdots & a_{n-2} \\ \vdots & \vdots & \vdots & \ddots & \vdots \\ a_n & a_{n-1} & a_{n-2} & \cdots & a_0 \end{bmatrix}.$$

Putting $a_{-n} := a_n$, the associated Fourier series

$$f(t) = \sum_{n=-\infty}^{\infty} a_n e^{int} = a_0 + 2 \sum_{n=1}^{\infty} a_n \cos(nt), \quad t \in [0, 2\pi]$$

is real valued and we have

$$\min f \leq \lambda \leq \max f$$

for each $n \in \mathbb{Z}_{\geq 0}$ and each $\lambda \in \text{Spec}(A_n)$.

Proof. See [13, Lemma 4.1]. □

This result yields an upper bound for the maximal eigenvalue of the matrix A : as the associated Fourier series is given by

$$f(t) = a_0 + 2 \sum_{n=1}^{\infty} a_n \cos(nt), \quad t \in [0, 2\pi],$$

and because all $a_n > 0$, the series attains its maximum when all the cosines are 1. In fact, the proof can be slightly modified to obtain the following stronger result:

$$\lambda_{\max}(A(N, 1)) \leq a_0 + 2 \sum_{n=1}^N a_n,$$

by only considering the truncated Fourier series.

A classical lower bound of the maximal eigenvalue of the matrix A is given by

$$\frac{S}{N+1} \leq \lambda_{\max}(A(N, 1)),$$

where S is the sum of all entries in the matrix $A(N, 1)$ [11]. For us,

$$\frac{S}{N+1} = a_0 + 2 \left(\frac{N}{N+1} a_1 + \frac{N-1}{N+1} a_2 + \frac{N-2}{N+1} a_3 + \dots + \frac{1}{N+1} a_N \right).$$

Using the upper bound and the fact that $a_n \rightarrow 0$, we see that both bounds are sharp fairly fast and we have demonstrated the following:

Lemma 3.13 (Asymptotic maximal eigenvalue for $K = 1$). *For a given N , we have that the maximal eigenvalue of A can be bounded above and below:*

$$a_0 + 2 \left(\frac{N}{N+1} a_1 + \frac{N-1}{N+1} a_2 + \frac{N-2}{N+1} a_3 + \dots + \frac{1}{N+1} a_N \right) \leq \lambda_{\max}(A(N, 1)) \leq a_0 + 2 \sum_{n=1}^N a_n.$$

In particular,

$$\lim_{N \rightarrow \infty} \lambda_{\max}(A(N, 1)) = a_0 + 2 \sum_{n=1}^{\infty} a_n.$$

Let us simplify this sum. We start by investigating the following sequence of partial sums:

Lemma 3.14. *Given $N \geq 1$, we have that*

$$\begin{aligned} \sum_{n=1}^N 2^{-n/2} (1 + 2^n) \ln(1 + 2^n) &= \frac{2^{-N/2}(\sqrt{2} - 1)}{3 - 2\sqrt{2}} (2^{N/2} - 1) + \sum_{n=1}^N \iota_n \\ &+ \frac{\ln 2}{3 - 2\sqrt{2}} \left(2\sqrt{2} + 2^{N/2}\sqrt{2} \left((\sqrt{2} - 1)N - 1 \right) - 2^{-N/2} \left(\sqrt{2} + (\sqrt{2} - 1)N \right) \right). \end{aligned}$$

The terms ι_n are integrals given by

$$\iota_n = \int_0^1 \frac{2^{-n/2}(1-x)}{x+2^n} dx > 0.$$

Proof. The central insight is to rewrite the $\ln(1 + 2^n)$ factor in the sum by integrating $1/(x + 2^n)$:

$$\begin{aligned} 2^{-n/2} (1 + 2^n) \ln(1 + 2^n) &= 2^{-n/2} (1 + 2^n) \left(\ln(2^n) + \int_0^1 \frac{dx}{x + 2^n} \right) \\ &= \ln(2) \left(n2^{-n/2} + n2^{n/2} \right) + \int_0^1 \frac{2^{-n/2}(1 + 2^n)}{x + 2^n} dx \\ &= \ln(2)n \left(2^{-n/2} + 2^{n/2} \right) + 2^{-n/2} + \int_0^1 \frac{2^{-n/2}(1-x)}{x + 2^n} dx. \end{aligned}$$

From here on, it can be verified that

$$\begin{aligned} \sum_{n=1}^N n \left(2^{-n/2} + 2^{n/2} \right) &= \\ \frac{1}{3 - 2\sqrt{2}} \left(2\sqrt{2} + 2^{N/2}\sqrt{2} \left((\sqrt{2} - 1)N - 1 \right) - 2^{-N/2} \left(\sqrt{2} + (\sqrt{2} - 1)N \right) \right) \end{aligned}$$

and

$$\sum_{n=1}^N 2^{-n/2} = \frac{2^{-N/2}(\sqrt{2} - 1)}{3 - 2\sqrt{2}} (2^{N/2} - 1).$$

□

Using this lemma, we can write the partial sums $\sum_{n=1}^N a_n$ in a closed form expression (in terms of square roots and logarithms), plus (a multiple of) this sum of integrals² $\sum_{n=1}^N \iota_n$.

²which, to the best of our knowledge, does not admit a nice analytical form.

Lemma 3.15. *Given $N \geq 1$, we can write the partial sum $\sum_{n=1}^N a_n$ as*

$$\sum_{n=1}^N a_n = \alpha + \beta_N + \gamma_N + (3 - 2\sqrt{2}) \sum_{n=1}^N \iota_n,$$

where we have grouped constant terms

$$\alpha = \sqrt{2} - 1 - (2 + \sqrt{2}) \ln 2 + 3 \ln 3 \approx 1.3435,$$

and terms that exponentially decay to zero as $N \rightarrow \infty$:

$$\beta_N = 2^{-N/2} \left(1 - \sqrt{2} - (\sqrt{2} + 1) \ln 2 + \sqrt{2} \ln(1 + 2^{-N}) - \ln(1 + 2^{-N-1}) \right)$$

and

$$\gamma_N = 2^{N/2} \sqrt{2} \left(\ln(1 + 2^{-N}) - \sqrt{2} \ln(1 + 2^{-N-1}) \right),$$

with $\beta_N, \gamma_N < 0$. The terms ι_n are the integrals from Lemma 3.14.

Proof. We start with

$$\begin{aligned} \sum_{n=1}^N a_n &= \sum_{n=1}^N 2^{-n/2} \left((2^{n+1} - 2^n) \ln(2) - 2(2^{n-1} + 1) \ln(2^{n-1} + 1) \right. \\ &\quad \left. + 3(2^n + 1) \ln(2^n + 1) - (2^{n+1} + 1) \ln(2^{n+1} + 1) \right). \end{aligned}$$

In this sum, we can already extract the following sum of a finite geometric sequence:

$$\sum_{n=1}^N 2^{-n/2} (2^{n+1} - 2^n) \ln(2) = \frac{\sqrt{2}}{\sqrt{2} - 1} (2^{N/2} - 1) \ln 2. \quad (9)$$

The remaining terms are rewritten by applying a reindexing step. Here, we have to account for the beginning and end terms that get added or cut off during this reindexing step, as these are not negligible. We find that

$$\begin{aligned} \sum_{n=1}^N 2^{-n/2} 2(2^{n-1} + 1) \ln(2^{n-1} + 1) &= 2\sqrt{2} \ln 2 - 2^{-\frac{N+1}{2}} 2(2^N + 1) \ln(2^N + 1) \\ &\quad + \sum_{n=1}^N 2^{-\frac{n+1}{2}} 2(2^n + 1) \ln(2^n + 1) \end{aligned} \quad (10)$$

and similarly

$$\begin{aligned} \sum_{n=1}^N 2^{-n/2} (2^{n+1} + 1) \ln(2^{n+1} + 1) &= -3 \ln 3 + 2^{-N/2} (2^N + 1) \ln(2^N + 1) \\ &+ \sum_{n=1}^N 2^{-\frac{n-1}{2}} 2 (2^n + 1) \ln(2^n + 1). \end{aligned} \quad (11)$$

The only remaining terms are

$$\sum_{n=1}^N 2^{-n/2} 3 (2^n + 1) \ln(2^n + 1), \quad (12)$$

and these do not have to be reindexed. We currently have

$$\sum_{n=1}^N a_n = (9) - (10) - (11) + (12).$$

Let us focus on $-(10) - (11) + (12)$. These terms can be rewritten as

$$-(10) - (11) + (12) = B(N) + \sum_{n=1}^N 2^{-n/2} (1 + 2^n) \ln(1 + 2^n),$$

where we have collected the beginning and end terms from earlier as $B(N)$:

$$\begin{aligned} B(N) &= 3 \ln(3) - 2\sqrt{2} \ln(2) \\ &+ 2^{-N/2} \left(\sqrt{2} (2^N + 1) \ln(2^N + 1) - (2^{N+1} + 1) \ln(2^{N+1} + 1) \right). \end{aligned}$$

The remaining terms $\sum_{n=1}^N 2^{-n/2} (1 + 2^n) \ln(1 + 2^n)$ can be informally referred to as ‘the hard part’ and we have derived an expression for these in Lemma 3.14.

Finally, after some rewriting, the partial sum $\sum_{n=1}^N a_n$ can indeed be found to equal the expression in the statement of this Lemma 3.15.

β_N and γ_N exponentially decay to zero as $N \rightarrow \infty$: That $\beta_N < 0$ exponentially decays to zero is clear. To show the same is true for γ_N , we simply note that for large N ,

$$\ln(1 + 2^{-N}) - \sqrt{2} \ln(1 + 2^{-N-1}) = \left(1 - \frac{1}{\sqrt{2}}\right) 2^{-N} + O(2^{-2N}),$$

so that premultiplication by something of the order of $2^{N/2}$ cannot prevent γ_N from exponentially decaying to zero as $N \rightarrow \infty$. \square

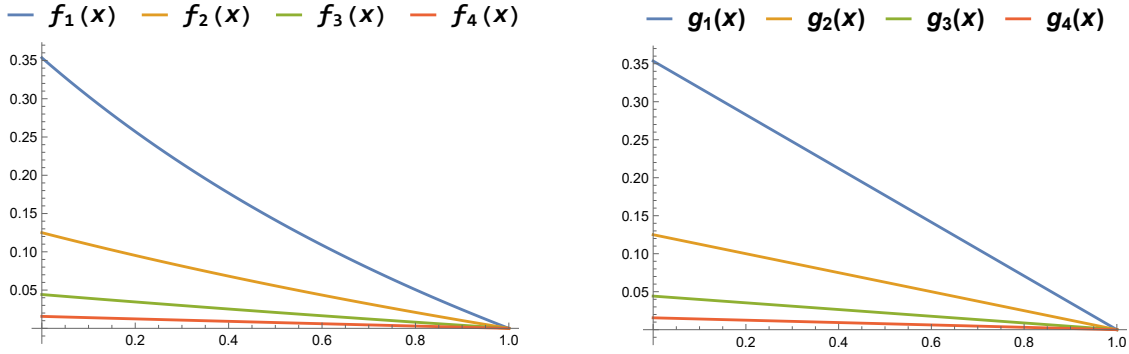


Figure 8: The first four functions $f_n(x) = \frac{2^{-n/2}(1-x)}{x+2^n}$ together with their linear upper bounds $g_n(x) = 2^{-3n/2}(1-x)$.

Combining Lemmas 3.13 to 3.15, we find the following:

Proposition 3.16. *The asymptotic maximal eigenvalue approaches*

$$\lim_{N \rightarrow \infty} \lambda_{\max}(A(N, 1)) = \ln\left(\frac{1024}{729}\right) + 2\alpha + 2(3 - 2\sqrt{2}) \sum_{n=1}^{\infty} \iota_n \approx 3.1105202.$$

Remark 3.17. This is already

$$3.11052/\pi = 99.01\%$$

of the way to π ; but as could be expected, we do not fully approach it.

Nevertheless, it is remarkable how closely we can approximate π even with just $K = 1$, suggesting that the parameter K , which governs the number of horizontal translates of the Haar wavelets being employed, plays a less significant role than N , which controls the fineness of the wavelets.

That we indeed cannot fully get to π can be made clear by considering a specific upper bound for the series of integrals. Recall that

$$\iota_n = \int_0^1 f_n,$$

where

$$f_n(x) = \frac{2^{-n/2}(1-x)}{x+2^n}, \quad x \in [0, 1].$$

These functions are all positive, decreasing, (slightly) convex and their graphs connect the points $(0, 2^{-3n/2})$ and $(1, 0)$, as can be observed in Fig. 8. As such, these functions can be dominated by the following sequence of linear functions:

$$g_n(x) = 2^{-3n/2}(1-x), \quad x \in [0, 1],$$

with corresponding integrals

$$\kappa_n = \int_0^1 g_n = 2^{-1-\frac{3n}{2}}.$$

It follows that the asymptotic maximal eigenvalue has the following *exact* (in terms of square roots and logarithms of whole numbers) upper bound:

$$\begin{aligned} M_0 &= \ln \left(\frac{1024}{729} \right) + 2\alpha + 2(3 - 2\sqrt{2}) \sum_{n=1}^{\infty} \kappa_n \\ &= 2(3 - \sqrt{2}) \ln 2 + \frac{18\sqrt{2} - 19}{7} \\ &\approx 3.12063, \end{aligned}$$

demonstrating that we indeed do not get to π .

Sharper upper bounds may be found by computing the first N integrals ι_n exactly and bounding the rest ($n \geq N + 1$) by κ_n :

$$M_N = \ln \left(\frac{1024}{729} \right) + 2\alpha + 2(3 - 2\sqrt{2}) \left(\sum_{n=1}^N \iota_n + \sum_{n=N+1}^{\infty} \kappa_n \right).$$

For example:

$$\begin{aligned} M_1 &= \frac{64 - 33\sqrt{2}}{28} + (18 - 11\sqrt{2}) \ln 2 + 3(-4 + 3\sqrt{2}) \ln 3 \approx 3.11248, \\ M_2 &= \frac{60\sqrt{2} - 61}{56} + 5(2\sqrt{2} - 3) \ln 5 + 3(3\sqrt{2} - 4) \ln 6 \approx 3.11088, \end{aligned}$$

and so on.

In general, one indeed has the following result, which is a corollary of the fundamental eigenvalue distribution theorem of Szegő: (Originally stated in [14], see also [8, Theorem 1.1], [9, Theorem 1] and [13, Theorem 4.2, Corollary 4.2].)

Theorem 3.18 (Corollary of Szegő's Fundamental Eigenvalue Distribution Theorem). *Let $(a_n)_{n \geq 0}$ be an absolutely summable sequence in \mathbb{C} and define an associated sequence of Hermitian Toeplitz matrices*

$$A_n = \begin{bmatrix} a_0 & a_1^* & a_2^* & \cdots & a_n^* \\ a_1 & a_0 & a_1^* & \cdots & a_{n-1}^* \\ a_2 & a_1 & a_0 & \cdots & a_{n-2}^* \\ \vdots & \vdots & \vdots & \ddots & \vdots \\ a_n & a_{n-1} & a_{n-2} & \cdots & a_0 \end{bmatrix}.$$

Putting $a_{-n} := a_n^*$, the Fourier series

$$f(t) = \sum_{n=-\infty}^{\infty} a_n e^{int}, \quad t \in [0, 2\pi]$$

is real valued and we have

$$\begin{aligned} \lim_{n \rightarrow \infty} \lambda_{\max}(A_n) &= \max f \\ \lim_{n \rightarrow \infty} \lambda_{\min}(A_n) &= \min f, \end{aligned}$$

where $\lambda_{\max}(A_n)$ increases with n and $\lambda_{\min}(A_n)$ decreases with n .

3.5.2 Outlook: The general case $K \geq 1$

For general K , the matrix A is no longer necessarily Toeplitz, but block Toeplitz. Luckily, for block Toeplitz matrices we have the following natural generalization of Szegő's Theorem 3.18: (See also [8, Corollary 3.5] and [9, Theorem 3])

Theorem 3.19 (Corollary of Szegő's theorem for block Toeplitz matrices). *Let $(A_n)_{n \geq 0}$ be a sequence of matrices in $\mathbb{C}^{K \times K}$ such that for all $k, l \in \{1, \dots, K\}$ we have that the sequence $((A_n)_{k,l})_{n \geq 0}$ is absolutely summable in \mathbb{C} and consider the sequence of Hermitian block Toeplitz matrices*

$$\mathcal{A}_n = \begin{bmatrix} A_0 & A_1^* & A_2^* & \cdots & A_n^* \\ A_1 & A_0 & A_1^* & \cdots & A_{n-1}^* \\ A_2 & A_1 & A_0 & \cdots & A_{n-2}^* \\ \vdots & \vdots & \vdots & \ddots & \vdots \\ A_n & A_{n-1} & A_{n-2} & \cdots & A_0 \end{bmatrix} \in \mathbb{C}^{(n+1)K \times (n+1)K}.$$

Putting $A_{-n} = A_n^*$, the $K \times K$ matrix valued Fourier series

$$F(t) = \sum_{n=-\infty}^{\infty} A_n e^{int}, \quad t \in [0, 2\pi]$$

is Hermitian and we have

$$\begin{aligned} \lim_{n \rightarrow \infty} \lambda_{\max}(\mathcal{A}_n) &= \max_{t \in [0, 2\pi]} \lambda_{\max}(F(t)) \\ \lim_{n \rightarrow \infty} \lambda_{\min}(\mathcal{A}_n) &= \min_{t \in [0, 2\pi]} \lambda_{\min}(F(t)). \end{aligned}$$

Similarly as in Proposition 3.12, we also have that these asymptotics for the extreme eigenvalues are effective bounds on all eigenvalues: for each $n \in \mathbb{Z}_{\geq 0}$ and each $\lambda \in \text{Spec}(\mathcal{A}_n)$, we have

$$\min_{t \in [0, 2\pi]} \lambda_{\min}(F(t)) \leq \lambda \leq \max_{t \in [0, 2\pi]} \lambda_{\max}(F(t)).$$

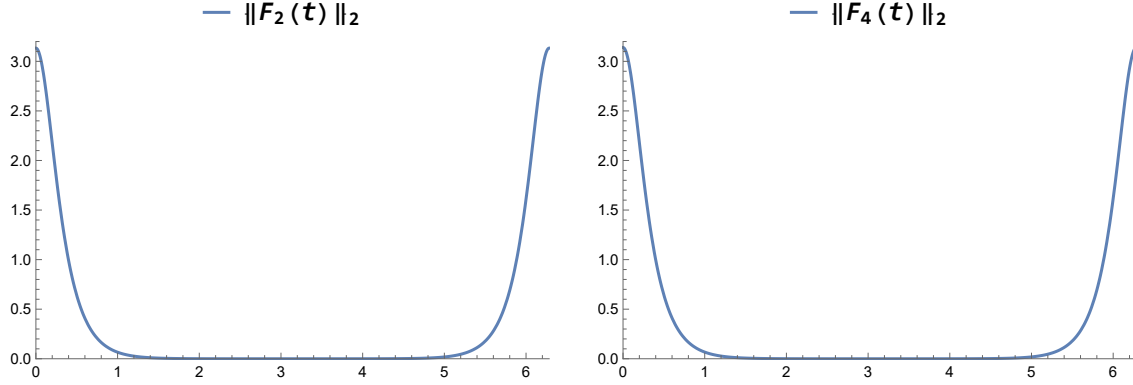


Figure 9: The graphs of $\lambda_{\max}(F_2(t))$ and $\lambda_{\max}(F_4(t))$. The graphs corresponding to different values of K are very similar.

Let us define $F_K(t)$ as the $K \times K$ matrix valued Fourier series

$$F_K(t) = \sum_{n=-\infty}^{\infty} A_n(K)e^{int}, \quad t \in [0, 2\pi].$$

According to Theorem 3.19, we have the result

$$\lim_{N \rightarrow \infty} \lambda_{\max}(A(N, K)) = \max_{t \in [0, 2\pi]} \lambda_{\max}(F_K(t)).$$

The situation here is considerably more complex than the special case $K = 1$, as we now need to compute the maximal eigenvalue of a matrix valued Fourier series (which is trivial only in the case of a 1×1 matrix). Nonetheless, we conjecture that for any $K \geq 1$, similar to the case $K = 1$, the maximum is achieved at $t = 0$:

$$\max_{t \in [0, 2\pi]} \lambda_{\max}(F_K(t)) = \lambda_{\max}(F_K(0)).$$

Fig. 9 shows the function $\lambda_{\max}(F_K(t))$ for the values $K = 2$ and $K = 4$, providing numerical evidence of the fact that the maximum is indeed achieved at $t = 0$. The graphs for higher values of K are visually indistinguishable, though the maximum gets closer and closer to π .

Remark 3.20. In addition, we remark that it is not necessary to prove that the maximum is achieved at $t = 0$. It suffices to show

$$\lambda_{\max}(F_K(0)) \longrightarrow \pi,$$

as this would directly imply

$$\max_{t \in [0, 2\pi]} \lambda_{\max}(F_K(t)) \longrightarrow \pi.$$

K	$\lambda_{\max}(F_K(0))$	K	$\lambda_{\max}(F_K(0))$	K	$\lambda_{\max}(F_K(0))$
1	3.1105201	21	3.1415124	41	3.1415717
2	3.1330806	22	3.1415195	42	3.1415727
3	3.1377294	23	3.1415258	43	3.1415736
4	3.1394026	24	3.1415312	44	3.1415745
5	3.1401857	25	3.1415360	45	3.1415753
6	3.1406136	26	3.1415403	46	3.141576
7	3.1408725	27	3.1415441	47	3.1415768
8	3.1410408	28	3.1415475	48	3.1415774
9	3.1411564	29	3.1415506	49	3.1415780
10	3.1412391	30	3.1415534	50	3.1415786
11	3.1413004	31	3.1415559	51	3.1415792
12	3.1413470	32	3.1415581	52	3.1415797
13	3.1413833	33	3.1415602	53	3.1415802
14	3.1414121	34	3.1415621	54	3.1415807
15	3.1414354	35	3.1415638	55	3.1415811
16	3.1414544	36	3.1415654	56	3.1415815
17	3.1414702	37	3.1415669	57	3.1415819
18	3.1414834	38	3.1415682	58	3.1415823
19	3.1414946	39	3.1415694	59	3.1415826
20	3.1415042	40	3.1415706	60	3.1415830

Table 2: Numerical evidence for $\lambda_{\max}(F_K(0)) \rightarrow \pi$ as $K \rightarrow \infty$.

To establish this, it is enough to prove that for any small $\delta > 0$, we can find a sufficiently large $K \geq 1$ such that $\pi - \delta < \lambda_{\max}(F_K(0))$. (The reason why is similar to the argument presented in Remark 3.10.)

For reference, the $K \times K$ matrix valued series $F_K(0)$ is the sum

$$F_K(0) = \sum_{n=-\infty}^{\infty} A_n(K) = A_0(K) + \sum_{n=1}^{\infty} (A_n(K) + A_n^T(K)).$$

Numerical experiments clearly suggest that indeed

$$\lambda_{\max}(F_K(0)) \longrightarrow \pi$$

as $K \rightarrow \infty$, see Table 2. As a self-consistency check, we note the correspondence between the exact asymptotic eigenvalue in the special case $K = 1$ obtained in Proposition 3.16 and the one estimated in Table 2.

Remark 3.21. For the numerical experiments (Fig. 9 and Table 2) we approximate $F_K(t)$ by the partial sum

$$\sum_{n=-50}^{50} A_n(K) e^{int}.$$

In particular, $F_K(0)$ is approximated by

$$A_0(K) + \sum_{n=1}^{50} (A_n(K) + A_n^T(K)).$$

Outlook 3.22. Although a formal proof for $\lambda_{\max}(F_K(0)) \longrightarrow \pi$ as $K \rightarrow \infty$ currently eludes us, we hope that it can be done with the appropriate mathematical tools.

4 Bumpification (Step 2)

Assume now that for a given $\eta \in (\sqrt{2} - 1, 1)$, we can find a resolution $\{N_0, N_1, K\}$ and initial test functions, in terms of Haar wavelets (3), which present an exact solution to the system of equations (2). That is, in this section we *assume* Conjecture A is true, and demonstrate that these initial test functions can be transformed into continuous and differentiable versions consistent with the smoothness requirements of QFT.

The process is as follows: In Section 4.1, we introduce C^∞ versions of the Haar wavelets by smoothing out their points of discontinuity, using a small tuning parameter $\varepsilon > 0$. Then, in Section 4.2, we demonstrate that by choosing ε sufficiently small, these “bumpified” Haar wavelets closely approximate the original wavelets (in the appropriate sense). This ensures that, after substituting the C^∞ wavelets for the original ones in the expansion (3), the system of equations (2) remains satisfied up to the desired degree of precision.

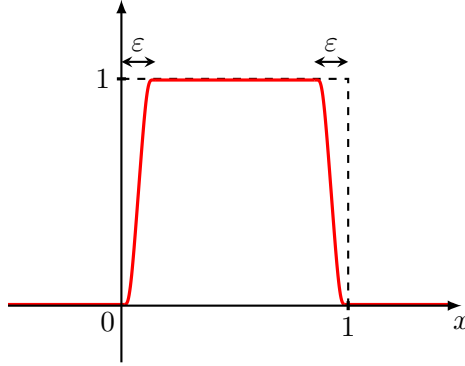


Figure 10: The basic Planck-taper window function s^ε .

4.1 Bumpified Haar wavelets

To construct smooth “bumpified” versions of the Haar wavelets (still compactly supported), following [10], the authors of [12] employ the *Planck-taper window function*.

Definition 4.1. The *basic Planck-taper window function* with support on the interval $[0, 1]$ is defined by

$$s^\varepsilon(x) = \begin{cases} \left[1 + \exp\left(\frac{\varepsilon(2x - \varepsilon)}{x(x - \varepsilon)}\right) \right]^{-1} & \text{if } 0 < x < \varepsilon \\ 1 & \text{if } \varepsilon \leq x \leq 1 - \varepsilon \\ s^\varepsilon(1 - x) & \text{if } 1 - \varepsilon < x < 1 \\ 0 & \text{otherwise.} \end{cases}$$

Here, $\varepsilon > 0$ is a sufficiently small tuning parameter.

This function is the C^∞ version of the ‘basic rectangle’,

$$r(x) = \begin{cases} 1 & \text{if } 0 \leq x < 1 \\ 0 & \text{otherwise,} \end{cases}$$

smoothing over the point of discontinuity $x = 0$ by making use of the transition function $x \mapsto \left[1 + \exp\left(\frac{\varepsilon(2x - \varepsilon)}{x(x - \varepsilon)}\right) \right]^{-1}$, and symmetrically for the other ‘problematic point’ $x = 1$. See Fig. 10.

The deviation between the window function s^ε and the basic rectangle r can be made arbitrarily small by tuning ε . In fact, if we measure this deviation using any L^p norm (except L^∞), we find that it is proportional to the tuning parameter ε .

Proposition 4.2. *Let $1 \leq p < \infty$ and write $\|\cdot\|_p$ for the L^p norm. Then,*

$$\|r - s^\varepsilon\|_p^p = \alpha_p \varepsilon \leq \varepsilon,$$

where

$$\alpha_p := 2 \int_0^1 \left(1 - \frac{1}{1 + \exp\left(\frac{2y-1}{y(y-1)}\right)} \right)^p dy \in (0, 1].$$

Proof. As r and s^ε differ only on the intervals $(0, \varepsilon)$ and $(1 - \varepsilon, 1)$, we have

$$\begin{aligned} \|r - s^\varepsilon\|_p^p &= \int_0^\varepsilon |r(x) - s^\varepsilon(x)|^p dx + \int_{1-\varepsilon}^1 |r(x) - s^\varepsilon(x)|^p dx \\ &= 2 \int_0^\varepsilon |r(x) - s^\varepsilon(x)|^p dx. \end{aligned}$$

Now, substituting $y = x/\varepsilon$ indeed yields

$$\|r - s^\varepsilon\|_p^p = 2 \int_0^1 \left(1 - \frac{1}{1 + \exp\left(\frac{2y-1}{y(y-1)}\right)} \right)^p \varepsilon dy = \alpha_p \varepsilon.$$

To prove that this constant satisfies $0 < \alpha_p \leq 1$, we simply note that α_p is decreasing in p and so it is maximal for $p = 1$, where we have $\alpha_1 = 1$. The latter observation follows from

$$\int_0^1 \left(1 - \frac{1}{1 + \exp\left(\frac{2y-1}{y(y-1)}\right)} \right) dy = \frac{1}{2}.$$

□

Remark 4.3. It is a standard result in real analysis that the limit function of a uniformly convergent sequence of continuous functions remains continuous. Hence, Proposition 4.2 trivially fails for $p = \infty$, since an L^∞ converging sequence of continuous functions is a uniformly convergent sequence of functions, but the candidate limit function r is discontinuous.

Using the window function s^ε , we can define the C^∞ version of the mother Haar wavelet ψ , by similarly smoothing over its points of discontinuity. See Fig. 11.

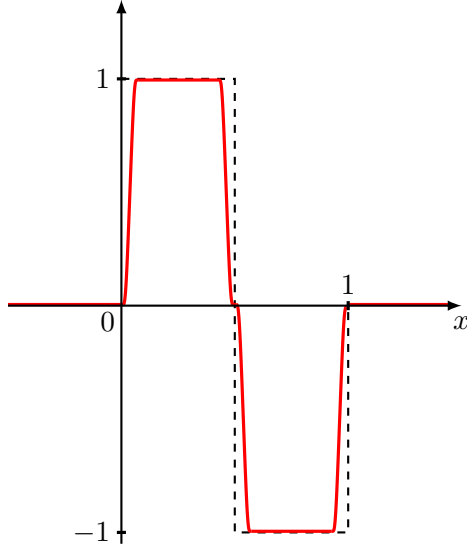


Figure 11: The mother bumpified Haar wavelet $\sigma^\varepsilon = \sigma_{0,0}^\varepsilon$.

Definition 4.4 (Bumpified Haar wavelets). The *mother bumpified Haar wavelet* with support on $[0, 1]$ is defined by

$$\sigma^\varepsilon(x) = \begin{cases} +s^\varepsilon(2x) & \text{if } 0 \leq x < \frac{1}{2} \\ -s^\varepsilon(2x - 1) & \text{if } \frac{1}{2} \leq x < 1 \\ 0 & \text{otherwise.} \end{cases}$$

Bumpified versions of the Haar wavelets $\psi_{n,k}$ may then be defined by

$$\sigma_{n,k}^\varepsilon(x) = \begin{cases} 2^{n/2} \sigma^\varepsilon(2^n x - k) & \text{if } x \in I_{n,k} \\ 0 & \text{otherwise.} \end{cases}$$

Analogously as in Proposition 4.2 we can control the deviation between $\psi_{n,k}$ and $\sigma_{n,k}$ by tuning ε . In fact, the bounds are very similar.

Proposition 4.5. *Let $1 \leq p < \infty$. Then,*

$$\|\psi - \sigma^\varepsilon\|_p^p = \alpha_p \varepsilon \leq \varepsilon.$$

Furthermore, for all $k, n \in \mathbb{Z}$ we have

$$\|\psi_{n,k} - \sigma_{n,k}^\varepsilon\|_p^p = 2^{\frac{n}{2p} - n} \alpha_p \varepsilon \leq 2^{-n/2} \varepsilon.$$

Proof. Using that

$$\psi(x) = \begin{cases} +r(2x) & \text{if } 0 \leq x < \frac{1}{2} \\ -r(2x-1) & \text{if } \frac{1}{2} \leq x < 1 \\ 0 & \text{otherwise,} \end{cases}$$

by applying appropriate substitutions we can identify $\|\psi - \sigma^\varepsilon\|_p^p$ as $\|r - s^\varepsilon\|_p^p$:

$$\begin{aligned} \|\psi - \sigma^\varepsilon\|_p^p &= \int_0^{1/2} |r(2x) - s^\varepsilon(2x)|^p dx + \int_{1/2}^1 |r(2x-1) - s^\varepsilon(2x-1)|^p dx \\ &= \frac{1}{2} \int_0^1 |r(y) - s^\varepsilon(y)|^p dy + \frac{1}{2} \int_0^1 |r(y) - s^\varepsilon(y)|^p dy \\ &= \|r - s^\varepsilon\|_p^p. \end{aligned}$$

Similarly, applying the substitution $y = 2^n x - k$ yields

$$\begin{aligned} \|\psi_{n,k} - \sigma_{n,k}^\varepsilon\|_p^p &= \int_{I_{n,k}} |2^{n/2}\psi(2^n x - k) - 2^{n/2}\sigma^\varepsilon(2^n x - k)|^p dx \\ &= 2^{\frac{n}{2p}} \int_0^1 |\psi(y) - \sigma^\varepsilon(y)|^p \frac{dy}{2^n} \\ &= 2^{\frac{n}{2p} - n} \|\psi - \sigma^\varepsilon\|_p^p \\ &= 2^{\frac{n}{2p} - n} \|r - s^\varepsilon\|_p^p. \end{aligned}$$

Both results now follow from Proposition 4.2. □

Lemma 3.2 remains valid for these bumpified Haar wavelets, and the proof follows in a completely analogous manner.

Lemma 4.6. *For all $n, k \in \mathbb{Z}$ we have*

$$\sigma_{n,k}^\varepsilon(-x) = -\sigma_{n,-k-1}^\varepsilon(x).$$

4.2 The final test functions

The final step in the procedure is to replace each occurrence of the Haar wavelet $\psi_{n,k}(x)$ with its bumpified counterpart $\sigma_{n,k}^\varepsilon$ in the expansion (3) of the *initial* set of test functions $(\tilde{f}, \tilde{f}'), (\tilde{g}, \tilde{g}')$ obtained in Section 3, where we *assume* that these preliminary test functions satisfy the system of equations (2) exactly for a given $\eta \in (\sqrt{2} - 1)$ (so assuming

Conjecture A is true). Specifically, we define the new test functions as follows:

$$f_j^{(\varepsilon)}(x) = \sum_{n=N_0}^{N_1} \sum_{k=-K}^{-1} f_j(n, k) \sigma_{n,k}^\varepsilon(x), \quad \text{for } j \in \{1, 2\}, \quad (13)$$

with analogous expressions for the other test functions f' , g and g' . The key idea is that by taking $\varepsilon > 0$ sufficiently small, these new test functions remain close to being normalized and nearly satisfy the necessary inner product relations:

$$\langle f^{(\varepsilon)} | g^{(\varepsilon)} \rangle \approx \langle f'^{(\varepsilon)} | g^{(\varepsilon)} \rangle \approx \langle f^{(\varepsilon)} | g'^{(\varepsilon)} \rangle \approx -\langle f'^{(\varepsilon)} | g'^{(\varepsilon)} \rangle \approx -i \frac{\sqrt{2}\eta}{1 + \eta^2},$$

while still satisfying the smoothness conditions required for them to be valid test functions in the context of QFT. However, these test functions need to be *exactly* normalized, not just approximately. Therefore, we introduce the following normalization factors:

$$\begin{aligned} a^{(\varepsilon)} &:= \langle f^{(\varepsilon)} | f^{(\varepsilon)} \rangle^{-1}, & a'^{(\varepsilon)} &:= \langle f'^{(\varepsilon)} | f'^{(\varepsilon)} \rangle^{-1} \\ b^{(\varepsilon)} &:= \langle g^{(\varepsilon)} | g^{(\varepsilon)} \rangle^{-1}, & b'^{(\varepsilon)} &:= \langle g'^{(\varepsilon)} | g'^{(\varepsilon)} \rangle^{-1}. \end{aligned}$$

If ε is small, these factors should all be close to 1. We conclude by defining

$$a^{(\varepsilon)} f^{(\varepsilon)}, \quad a'^{(\varepsilon)} f'^{(\varepsilon)}, \quad b^{(\varepsilon)} g^{(\varepsilon)}, \quad b'^{(\varepsilon)} g'^{(\varepsilon)}$$

as our final set of test functions.

To demonstrate that the proposed method of substituting wavelets works, we have to prove the following limit:

Proposition 4.7. *We have*

$$\lim_{\varepsilon \rightarrow 0} \langle a^{(\varepsilon)} f^{(\varepsilon)} | b^{(\varepsilon)} g^{(\varepsilon)} \rangle = -i \frac{\sqrt{2}\eta}{1 + \eta^2},$$

and similar for the other three inner products.

Since

$$\langle a^{(\varepsilon)} f^{(\varepsilon)} | b^{(\varepsilon)} g^{(\varepsilon)} \rangle = a^{(\varepsilon)} b^{(\varepsilon)} \langle f^{(\varepsilon)} | g^{(\varepsilon)} \rangle,$$

and similar for the other inner products, it is sufficient to prove the following two statements:

- The normalization constants $a^{(\varepsilon)}$, $b^{(\varepsilon)}$, $a'^{(\varepsilon)}$ and $b'^{(\varepsilon)}$ converge to 1 as $\varepsilon \rightarrow 0$.
- $\lim_{\varepsilon \rightarrow 0} \langle f^{(\varepsilon)} | g^{(\varepsilon)} \rangle = -i \frac{\sqrt{2}\eta}{1 + \eta^2}$, and similar for the other inner products.

These statements are proved in Lemmas 4.8 and 4.9.

Lemma 4.8. *We have*

$$\lim_{\varepsilon \rightarrow 0} a^{(\varepsilon)} = 1,$$

and similar for the other three normalization factors.

Proof. It suffices to show that

$$\lim_{\varepsilon \rightarrow 0} \langle f^{(\varepsilon)} \mid f^{(\varepsilon)} \rangle = 1.$$

To do this, we make use of the assumption that the preliminary test functions are already normalized and expand:

$$\begin{aligned} \left| \langle f^{(\varepsilon)} \mid f^{(\varepsilon)} \rangle - 1 \right| &= \left| \langle f^{(\varepsilon)} \mid f^{(\varepsilon)} \rangle - \langle \tilde{f} \mid \tilde{f} \rangle \right| \\ &= \left| \int \left(f_1^{(\varepsilon)2} - \tilde{f}_1^2 + f_2^{(\varepsilon)2} - \tilde{f}_2^2 \right) dx \right| \\ &\leq \int \left| f_1^{(\varepsilon)2} - \tilde{f}_1^2 \right| dx + \int \left| f_2^{(\varepsilon)2} - \tilde{f}_2^2 \right| dx. \end{aligned}$$

Here,

$$\begin{aligned} \int \left| f_1^{(\varepsilon)2} - \tilde{f}_1^2 \right| dx &= \int \left| (f_1^{(\varepsilon)} + \tilde{f}_1)(f_1^{(\varepsilon)} - \tilde{f}_1) \right| dx \\ &\leq \max \left| f_1^{(\varepsilon)} + \tilde{f}_1 \right| \int \left| f_1^{(\varepsilon)} - \tilde{f}_1 \right| dx \\ &= \max \left| f_1^{(\varepsilon)} + \tilde{f}_1 \right| \times \left\| f_1^{(\varepsilon)} - \tilde{f}_1 \right\|_1, \end{aligned}$$

with $f_1^{(\varepsilon)} + \tilde{f}_1$ a finite sum of ε -uniformly bounded functions and

$$\left\| f_1^{(\varepsilon)} - \tilde{f}_1 \right\|_1 \leq \sum_{n=N_0}^{N_1} \sum_{k=-K}^{-1} |f_1(n, k)| \left\| \sigma_{n,k}^\varepsilon - \psi_{n,k} \right\|_1 \longrightarrow 0 \quad \text{as } \varepsilon \rightarrow 0$$

by Proposition 4.5. It follows that

$$\int \left| f_1^{(\varepsilon)2} - \tilde{f}_1^2 \right| dx \longrightarrow 0 \quad \text{as } \varepsilon \rightarrow 0,$$

and, by using a similar argument,

$$\int \left| f_2^{(\varepsilon)2} - \tilde{f}_2^2 \right| dx \longrightarrow 0 \quad \text{as } \varepsilon \rightarrow 0.$$

This finishes the proof. □

Lemma 4.9. *We have*

$$\lim_{\varepsilon \rightarrow 0} \langle f^{(\varepsilon)} \mid g^{(\varepsilon)} \rangle = -i \frac{\sqrt{2}\eta}{1 + \eta^2},$$

and similar for the other three inner products.

Proof. Here, too, we make use of the assumption that the preliminary test functions are already normalized and expand:

$$\begin{aligned} \left| \langle f^{(\varepsilon)} \mid g^{(\varepsilon)} \rangle + i \frac{\sqrt{2}\eta}{1 + \eta^2} \right| &= \left| \langle f^{(\varepsilon)} \mid g^{(\varepsilon)} \rangle - \langle \tilde{f} \mid \tilde{g} \rangle \right| \\ &\leq \frac{1}{\pi} \sum_{n,k,m,\ell} \left| f_1(n,k)g_1(m,\ell) - f_2(n,k)g_2(m,\ell) \right| \\ &\quad \times \left| \iint \left(\frac{1}{x-y} \right) \left(\sigma_{n,k}^\varepsilon(x)\sigma_{m,\ell}^\varepsilon(y) - \psi_{n,k}(x)\psi_{m,\ell}(y) \right) dx dy \right|. \end{aligned}$$

As this is a finite sum, it suffices to show that for each n, k, m, ℓ contained in the relevant resolution $\{N_0, N_1, K\}$, we have

$$\lim_{\varepsilon \rightarrow 0} \left| \iint_{I_{n,k} \times I_{m,\ell}} \left(\frac{1}{x-y} \right) \left(\sigma_{n,k}^\varepsilon(x)\sigma_{m,\ell}^\varepsilon(y) - \psi_{n,k}(x)\psi_{m,\ell}(y) \right) dx dy \right| = 0.$$

This can be proved by applying the dominated convergence theorem to the following pointwise limit:

$$\lim_{\varepsilon \rightarrow 0} \frac{\sigma_{n,k}^\varepsilon(x)\sigma_{m,\ell}^\varepsilon(y)}{x-y} = \frac{\psi_{n,k}(x)\psi_{m,\ell}(y)}{x-y}.$$

Indeed, we can dominate the sequence of functions as follows:

$$\left| \frac{\sigma_{n,k}^\varepsilon(x)\sigma_{m,\ell}^\varepsilon(y)}{x-y} \right| \leq \frac{2^{n/2}2^{m/2}}{|x-y|},$$

since

$$\iint_{I_{n,k} \times I_{m,\ell}} \frac{2^{n/2}2^{m/2}}{|x-y|} dx dy < \infty.$$

□

References

- [1] John S. Bell. On the Einstein Podolsky Rosen paradox. *Physics Physique Fizika*, 1:195–200, 1964.

- [2] John F. Clauser, Michael A. Horne, Abner Shimony, and Richard A. Holt. Proposed Experiment to Test Local Hidden-Variable Theories. *Physical Review Letters*, 23:880–884, 1969.
- [3] Boris S. Tsirelson. Quantum generalizations of Bell’s inequality. *Letters in Mathematical Physics*, 4(2):93–100, 1980.
- [4] Stephen J. Summers and Reinhard Werner. Bell’s inequalities and quantum field theory. I. General setting. *Journal of Mathematical Physics*, 28(10):2440–2447, 1987.
- [5] Stephen J. Summers and Reinhard Werner. Bell’s inequalities and quantum field theory. II. Bell’s inequalities are maximally violated in the vacuum. *Journal of Mathematical Physics*, 28(10):2448–2456, 1987.
- [6] Stephen J. Summers and Reinhard Werner. Maximal violation of Bell’s inequalities is generic in quantum field theory. *Communications in Mathematical Physics*, 110:247–259, 1987.
- [7] Ingrid Daubechies. Orthonormal Bases of Compactly Supported Wavelets. *Communications on Pure and Applied Mathematics*, 41(7):909–996, 1988.
- [8] Michele Miranda Jr and Paolo Tilli. Asymptotic Spectra of Hermitian Block Toeplitz Matrices and Preconditioning Results. *SIAM Journal on Matrix Analysis and Applications*, 21:867–881, 2000.
- [9] Houcem Gazzah, Philip A. Regalia, and Jean-Pierre Delmas. Asymptotic eigenvalue distribution of block Toeplitz matrices and application to blind SIMO channel identification. *IEEE Transactions on Information Theory*, 47(3):1243–1251, 2001.
- [10] David J. A. McKechnan, Craig Robinson, and Bangalore S. Sathyaprakash. A tapering window for time-domain templates and simulated signals in the detection of gravitational waves from coalescing compact binaries. *Classical and Quantum Gravity*, 27:084020, 2010.
- [11] Jacques Bénasséni. Lower bounds for the largest eigenvalue of a symmetric matrix under perturbations of rank one. *Linear and Multilinear Algebra*, 2011.
- [12] David Dudal, Philippe De Fabritiis, Marcelo S. Guimaraes, Itzhak Roditi, and Silvio P. Sorella. Maximal violation of the bell-clauser-horne-shimony-holt inequality via bumpified haar wavelets. *Physical Review D*, 108:L081701, 2023.
- [13] Robert M. Gray. *Toeplitz and Circulant Matrices: A Review*. Foundations and Trends in Communications and Information Theory. Now Publishers, 2006.
- [14] Ulf Grenander and Gabor Szegő. *Toeplitz Forms and Their Applications*. California monographs in mathematical sciences. University of California Press, 1958.

- [15] Rudolf Haag. *Local quantum physics: Fields, particles, algebras*. Springer Science & Business Media, 2012.
- [16] Gerald Kaiser. *A Friendly Guide to Wavelets*. Birkhauser Boston Inc., 1994.
- [17] Ülo Lepik and Helle Hein. *Haar Wavelets: With Applications*. Springer International Publishing, 2014.